



J. Serb. Chem. Soc. 91 (0) 1–13 (2026)
JSCS–13508

Adsorptive removal of Pb(II) from industrial effluent using nitric acid modified activated carbon: Optimization using Taguchi method

SAURABH MESHAM^{1*}, ANURADHA N JOSHI¹, GAUTAM PRASAD DEWANGAN¹,
CHANDRAKANT THAKUR² and ANUPAM B. SONI²

¹Department of Chemical Engineering, Guru Ghasidas Vishwavidyalaya, Bilaspur, 495009, Chhattisgarh, India and ²Department of Chemical Engineering, National Institute of Technology Raipur, 492010, Chhattisgarh, India

(Received 19 August, revised 22 October, accepted 25 December 2025)

Abstract: The study aimed to examine the use of nitric-acid-modified granular activated carbon to treat the wastewater of a lead-acid battery recycling unit for lead removal. The adsorbent was characterized using FTIR, SEM and XRD analyses. Surface functional groups, surface morphology and crystallinity were altered due to the modification. The batch adsorption study was conducted to evaluate the effects of adsorbent dose, initial pH, and contact time on adsorption performance for lead removal. Experiments were performed according to the Taguchi design of experiment method and factors were optimized based on SNR analysis to maximize the response. The ideal factor values were found to be pH 6, an adsorbent dose of 0.05 g, and a time of 240 min for the adsorption of lead onto the adsorbent, with an adsorbent uptake capacity of 9.93 mg g⁻¹. According to the ANOVA analysis, pH was found to be the most significant factor with an *F*-value of 28.07. Isotherm and kinetic studies were also carried out to understand the mechanism of adsorption. Adsorption was found to follow the Langmuir isotherm and the second order kinetic model.

Keywords: lead-acid battery; Taguchi optimization; adsorption; granular activated carbon; impregnation.

INTRODUCTION

Recycling of lead-acid batteries (LAB) is a crucial source of lead for storage battery production and also protects the environment. However, the recycling process generates wastewater with a pH of 1–1.5 and Pb concentrations ranging from 2 to 300 mg L⁻¹.¹ If this effluent is discharged untreated, it may adversely affect soil fertility and groundwater quality. If it enters the food chain, Pb may interfere with the functioning of major systems of the human body, such as the

*Corresponding author. E-mail: saurabhmeshram88@gmail.com
<https://doi.org/10.2298/JSC250819003M>

nervous system, digestive system, reproductive system, and urinary system by affecting major organs.² Conventionally, sodium carbonate is used to desulfurize and neutralize the effluent, separating the lead in the form of sludge.³ According to a 2011 market survey report by the Mineral Economics Division, Indian Bureau of Mines, there were only 316 registered recyclers in India in 2010, including five in the Chhattisgarh state. However, many backyard smelters dispose of effluent without any treatment to increase profits. These smelters require an efficient and inexpensive technique to treat the effluent and keep the Pb(II) concentration in the discharge within safe limits (0.1 mg L^{-1}).

Various methods are available to remove Pb(II) from water, such as precipitation, membrane separation, ion exchange, electrocoagulation, filtration and adsorption.⁴ Adsorption is a widely used technique due to its operational simplicity, cost-effectiveness and low capital cost. Activated carbon is often used in water treatment processes due to its different chemical characteristics, porous structure, and high surface area.⁵ Activated carbon is available in both powder (PAC) and granular (GAC) forms, with PAC having larger pores and GAC having smaller internal pores and a lower adsorption rate than PAC. GAC is preferred over PAC due to its ease of handling and disposal and reduced losses during operation.⁶ Several investigations have utilized GAC to treat wastewater, including removing lead from aqueous solutions by Dwivedi *et al.*, removing copper, zinc and lead ions by Chen and Wang, removing amoxicillin from water by Franco *et al.*, removing phenol from synthetic water by Sulaymon *et al.* and removing cadmium and lead by Jusoh *et al.*^{6–10}

Activated carbon is a widely used adsorbent for water treatment because of its porous structure, abundant active sites, functional groups, and high surface area. However, its adsorption capacity is limited, and researchers have modified it using chemical agents to enhance its efficiency by promoting chemisorption of pollutants on the surface. Wang *et al.* modified GAC with magnesium, resulting in an increased adsorption capacity from 3.47 to 8.08 mg g^{-1} for the adsorption of Cd(II).¹¹ Fan and Anderson used the manganese oxide for the removal of Cu(II) and Cd(II), and Yao *et al.* modified activated carbon derived from rice husk using nitric acid, which increased its uptake capacity by improving the surface characteristics and porous structure.^{12,13} In another study, Jiang *et al.* found that modifying activated carbon with HNO_3 as an impregnating agent after oxidizing it using concentrated sulfuric acid increased the mesoporous volume, specific surface area, and uptake capacity for the separation of dibenzothiophene and methylene blue.¹⁴

The modification of activated carbon with nitric acid has been widely; however, this study investigates the effect of modification on granular activated carbon. HNO_3 -modified GAC was used for the first as an adsorbent for the treatment of LAB recycling unit effluent. The characteristics of GAC and HNGAC were analyzed using SEM, FTIR and XRD to determine the effect of modification. The

adsorption experiments were conducted based on a Taguchi orthogonal L16 array (4^3) with four levels of the parameters: adsorbent dose, retention time and pH. The parameters were optimized using the signal-to-noise ratio (*SNR*) obtained from Taguchi analysis.

EXPERIMENTAL

Wastewater

The wastewater of a lead-acid battery (LAB) recycling plant was obtained from a smelter in Raipur, Chhattisgarh, India. The pH of the effluent was 1.2, and the concentration of Pb(II) was 11.2 mg L^{-1} . Prior to the batch adsorption study, the pH of the wastewater was adjusted using standard solutions of sodium hydroxide and hydrochloric acid.

Adsorbent

Granular activated carbon (GAC) was commercially procured and improved using nitric acid following the process described by El-Wakil *et al.*¹⁵ To prepare the modified GAC, a mixture of HNO_3 and distilled water in a 1:1 ratio was heated to $110 \text{ }^\circ\text{C}$. Then, 1 g of GAC was added to 5 mL of the heated solution and heated for 3 h. The resulting solution was filtered, and the solid fraction was collected and washed with distilled water until the pH reached 6. Finally, the nitric-acid-modified GAC (HNGAC) was dried for 24 h at $100 \text{ }^\circ\text{C}$ in a hot air oven.

Characterization

The surface functional groups of the adsorbents were analyzed using FTIR (Bruker, Alpha Model) within the $4000\text{--}400 \text{ cm}^{-1}$ range. The Zeiss EVO Series scanning electron microscope (SEM) was used to obtain surface micrographs and elemental composition of the adsorbents before and after the nitric acid modification. A PANalytical multifunctional XRD analyzer was used to obtain XRD spectra to determine the surface nature of the adsorbents. Standard ASTM methods were followed for proximate analysis.

Batch adsorption and optimization

A three factor, four level Taguchi L16 orthogonal array was obtained using Minitab 18.0 to perform the experiments. The three factors were initial pH of the wastewater (1.5, 3, 4.5, 6), dose ($0.1, 0.4, 0.7, 1.0 \text{ g (50 mL)}^{-1}$) and contact time (30, 60, 90, 240 min, Table I). For batch adsorption, a fixed amount of HNGAC was added to 250 ml of wastewater in an Erlenmeyer flask and kept in an orbital shaker for a defined time at $30 \text{ }^\circ\text{C}$ and 100 rpm. The Pb(II) concentration of the filtered effluent was analyzed using an atomic absorbance spectroscope (ECIL, India). Experimental runs were performed in duplicate and average values were reported. Eqs. (1) and (2) were used to determine the removal of Pb(II) and the uptake capacity of the adsorbent, respectively:

$$\text{Removal of Pb(II)} = 100 \frac{c_0 - c_e}{c_0} \quad (1)$$

$$q_e = \frac{c_0 - c_e}{m} V \quad (2)$$

where c_0 and c_e are the initial and final concentration of Pb(II) in the effluent, respectively. V is the volume of effluent and m is the mass of adsorbent.

Taguchi analysis, which uses a signal-to-noise ratio (*SNR*), was used to optimize the parameters and determine the optimal levels and their contribution to achieving the desired response.¹⁶ *SNR* analysis utilizes three response characteristic functions based on the minimization,

maximization and nominalization of the responses.¹⁷ In this study, a larger-the-better characteristic function was used for *SNR* analysis since the goal was to recover Pb(II), as represented:

$$\left(\frac{S}{N}\right)_{\text{Larger is better}} = -10 \log\left(\frac{1}{n} \sum_{i=1}^n \frac{1}{y_i^2}\right) \quad (3)$$

where y_i is the response and n is the number of experiments performed. The response factors were optimized using Minitab version 18.1. The significance and effect levels of the various factors in the batch adsorption study were determined using ANOVA analysis.

TABLE I. Batch adsorption parameters and their levels

Factor	Name	Level 1	Level 2	Level 3	Level 4
P	pH	1.5	3.0	4.5	6.0
D	Dose, g (50 mL) ⁻¹	0.1	0.4	0.7	1.0
T	Time, min	30	60	90	240

RESULTS AND DISCUSSION

Characterization

Fig. 1 shows a comparison of the FTIR spectra of GAC and HNGAC. After modification, the intensity of the surface functional group O–H, which corresponds to the peak at 3441 cm⁻¹ in GAC, increased and is represented by the peak at 3448 cm⁻¹ in HNGAC. The signal at 2926 cm⁻¹ in GAC indicates the presence of weakly bonded methyl and methylene groups (vibrational C–H bond). These C–H groups were oxidized and vanished from the HNGAC spectra following modification. It is evident that following modification, the peak at about 1630 cm⁻¹ in GAC, which is attributed to C=O groups, became noticeably more intense in HNGAC. The small peak in both spectra at around 1400 cm⁻¹ could be due to the presence of –CH₂ and –CH₃ groups. The peaks in the 1000–1200 cm⁻¹ region can be attributed to C–O stretching and O–H bending vibrations of ether, lactonic and phenol. The peak in the HNGAC spectrum at 607.50 cm⁻¹ may be due to newly formed surface groups of oxygen and nitrogen-containing groups.^{18–21}

In Fig. 2, SEM micrographs of GAC and HNGAC are presented. GAC has an irregular porous structure and a rough surface. Acid treatment with nitric acid decreased the internal micropores of GAC and removed impurities from its surface. Because nitric acid is a potent oxidant, the acid treatment created canal-like mesopores on the surface, which reduced the pore volume and surface area.^{22,23} The impregnation of nitric acid reduced the microporous pore volume and specific surface area of the activated carbon, as found by Jiang *et al.*²⁴ EDS elemental analysis showed that impurities from GAC were removed and oxygen-containing groups increased after acid treatment. Moreover, HNGAC was found to contain nitrogen, indicating that nitrogen-containing groups were formed on the surface after modification.

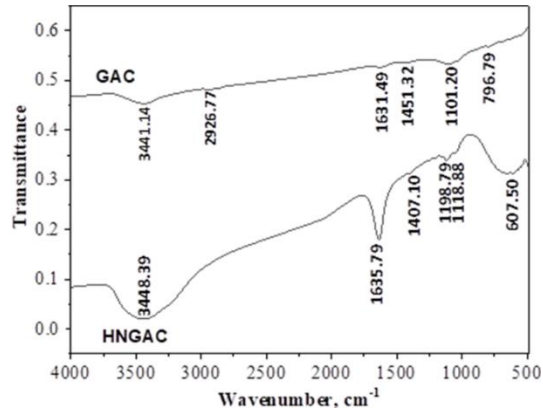


Fig. 1. FTIR spectra of GAC and HNGAC in the wavenumber range of 500–4000 cm^{-1} .

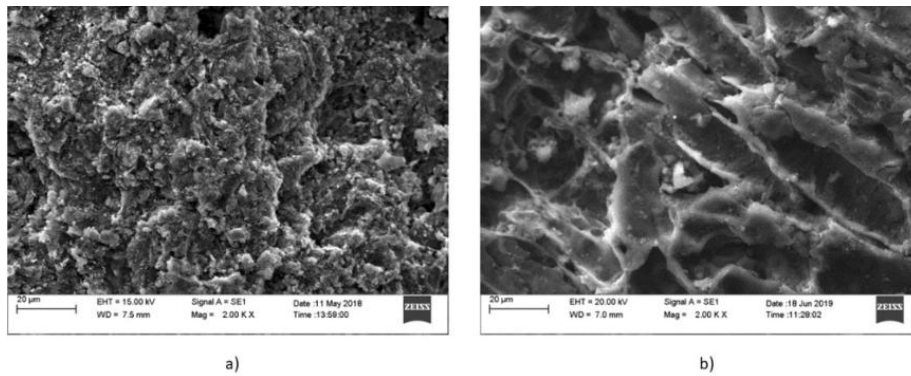


Fig. 2. Surface morphology images of: a) GAC and b) HNGAC obtained by SEM.

The crystalline or amorphous character of GAC and HNGAC was determined using the XRD spectra shown in Fig. 3. The peaks at 2θ 26 and 42° correspond to the (002) and (100) diffraction planes, respectively, and signify the amorphous

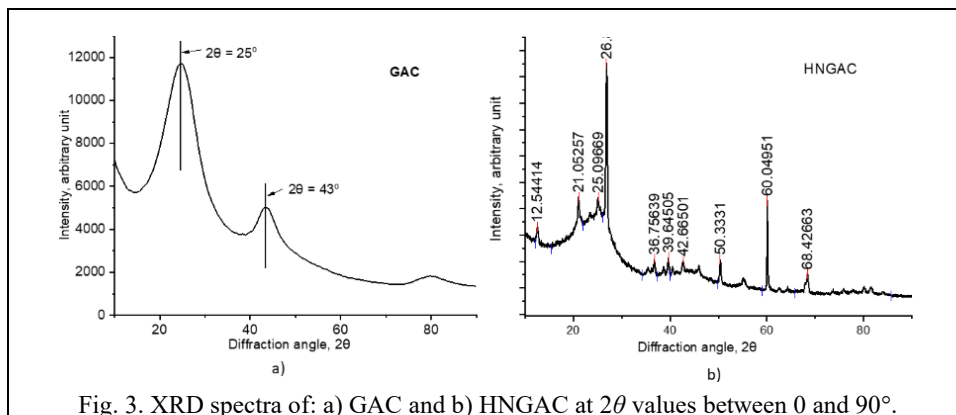


Fig. 3. XRD spectra of: a) GAC and b) HNGAC at 2θ values between 0 and 90° .

nature of activated carbon. The diffraction pattern of HNGAC exhibited several diffraction peaks, showing an increase in crystallinity due to modification. Similar effects of HNO₃ modification on adsorbent prepared from olive tree prune waste were observed by Calero *et al.*²⁵

Taguchi optimization

Three parameters at four different levels were used in the batch adsorption study using the Taguchi L16 orthogonal array. Table II displays the results for each run's adsorbent capacity and Fig. 4 displays the mean signal-to-noise ratio (*SNR*) plot for every variable associated with HNGAC's uptake capacity. It was found that while the *SNR* value decreased with increasing dose, it increased with increasing pH and time. At P4-D1-T4, the mean *SNR* value was highest. The optimal factor values were found to be pH 6, an adsorbent dose of 0.05 g, and a contact time of 240 min, based on the maximization feature of *SNR*. Nonetheless, there was little difference in uptake capacity for pH values of 4.5 and 6, so a pH value of 4.5 could be selected from an economic perspective for both adsorbents. The *SNR* analysis revealed that pH was the most influential factor in the adsorption of lead onto HNGAC.

TABLE II. Taguchi experimental runs for adsorption of lead onto HNGAC and the response variable (adsorbent uptake capacity)

Exp. No.	<i>P</i> (pH)	<i>D</i> (Dose, g)	<i>T</i> (Time, min)	$q_e / \text{mg g}^{-1}$
1	P1	D1	T1	0.12
2	P1	D2	T2	0.21
3	P1	D3	T3	0.20
4	P1	D4	T4	0.21
5	P2	D1	T2	2.38
6	P2	D2	T1	1.31
7	P2	D3	T4	0.95
8	P2	D4	T3	0.77
9	P3	D1	T3	9.43
10	P3	D2	T4	5.74
11	P3	D3	T1	3.18
12	P3	D4	T2	2.92
13	P4	D1	T4	9.93
14	P4	D2	T3	5.92
15	P4	D3	T2	3.96
16	P4	D4	T1	2.54

To determine the significance level of the factors on the adsorbent uptake capacity, an analysis of variance (ANOVA) was carried out and is presented in Table III. As observed, the coefficient of determination (R^2) was found to be 95.71, which signifies that the ANOVA model fitted well to the data. The ratio of variance between samples to variance within samples is termed the *F*-value and it indicates

the parameters which affect the response largely. The initial pH of the effluent was found to have the highest significance on the adsorption of lead onto HNGAC with an F -value of 28.07, whereas the least significant factor was adsorbent dose with an F -value of 0.007.

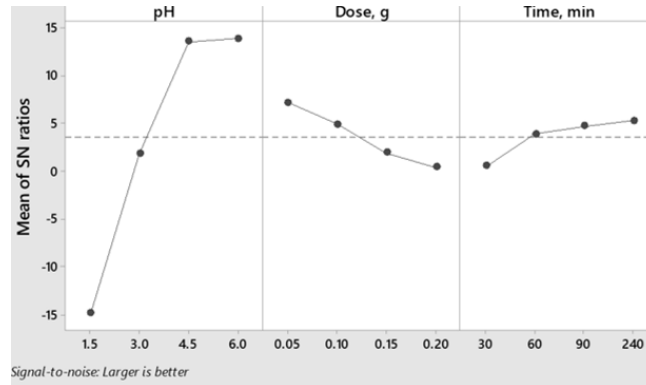


Fig. 4. Signal to noise ratio plot for the uptake capacity of HNGAC for pH, dose and time at different levels.

TABLE III. ANOVA analysis for adsorption of lead onto HNGAC

Source	DF	SS	MS	F -Value	P -Value
pH	3	90.629	30.210	28.07	0.001
Dose, g	3	35.563	11.854	11.01	0.007
Time, min	3	17.743	5.914	5.50	0.037
Error	6	6.457	1.076		
Total	15	150.393			
		R^2	$R^2(\text{adj})$		
		95.71 %	89.27 %		

Effect of each factor

The effect of pH on the adsorption of Pb(II) by HNGAC is shown in Fig. 5. The pH of the effluent has a significant impact on the adsorption process, affecting the charge on the surface and the ionization of Pb(II) in the effluent. To investigate this, the pH was varied from 1.5 to 6, as Pb(II) tends to precipitate at alkaline pH values.²⁶ At low pH values, Pb(II) and H^+ compete for adsorption onto HNGAC and consequently result in slow adsorption. Increasing the initial pH of the effluent led to an increase in the uptake capacity of HNGAC, as the competition between hydrogen and lead ions for adsorption sites decreased. Pb(II) ions were then able to bond with functional groups like $-OH$ and $-COOH$ present on the adsorbent surface.^{26,27} Moreover, at high pH, the negative charge on the surface increased, as protons are removed from the functional groups present on the surface, which results in enhanced electrostatic attraction for Pb(II), thereby improving adsorption.²⁸

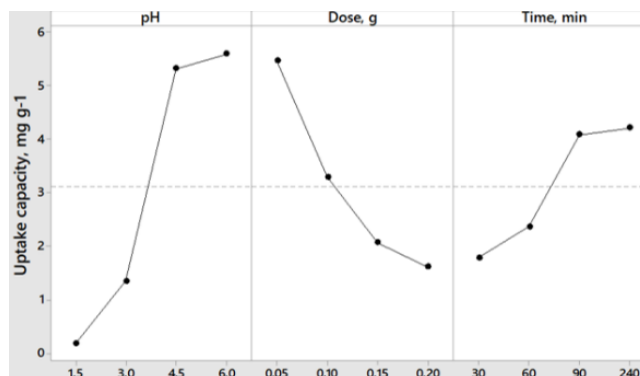


Fig. 5. Effect of initial pH, adsorbent dose and contact time on adsorption performance of HNGAC for the removal of Pb(II).

According to the results presented in Fig. 5, an increase in adsorbent dose led to a decrease in the uptake capacity of Pb(II). The reason behind this trend may be the existence of either unsaturated adsorption sites or overlapping and aggregation of adsorption sites due to maximum adsorption being reached at a certain dose of adsorbent.²⁹

The effect of contact time on Pb(II) uptake capacity was investigated, and as shown in Fig. 5, the uptake increased up to 90 min, after which it reached a plateau. This trend could be attributed to the initial availability of more than enough active sites for the adsorption of Pb(II), which became occupied over time, resulting in effective utilization of the adsorbent. As the number of active sites decreased with time, the competition between the lead ions in the effluent and the adsorbent surface for the remaining adsorption sites slowed down the adsorption process.

Fig. 6 displays response surface plots that illustrate the impact of two factors on the adsorption. Fig. 6a indicates that, to achieve optimal adsorbent capacity, adsorbent dose should be less than $0.1 \text{ g (50 mL)}^{-1}$, and the pH should exceed 4. This suggests that competition between Pb(II) and H^+ decreased at higher pH and that complete saturation of adsorption sites occurred at lower adsorbent doses. It can be found from Fig. 6b that higher adsorbent capacity is obtained at $\text{pH} > 4.5$ and $\text{time} > 80 \text{ min}$. This implies that insufficient interaction between the lead ions and adsorbent sites prevented high absorption capacity from being reached at the start of adsorption, even at high pH. High lead uptake capacity of HNGAC was achieved at doses $< 0.1 \text{ g/(50 mL)}$ and $\text{time} > 90 \text{ min}$ as can be observed in Fig. 6c.

Isotherm study

The fitting graphs for the Langmuir and Freundlich models fitted to the experimental data for Pb(II) adsorption onto HNGAC are shown in Fig. 7. Table IV displays the parameters of the isotherm models obtained from fitting the experimental data. The correlation coefficient (R^2) of the Langmuir model is higher than

that of the Freundlich model. This shows that the adsorption equilibrium data fit the Langmuir equation and the adsorption involves monolayer adsorption. The maximum monolayer adsorption capacity obtained from the Langmuir model is 9.93 mg g^{-1} for HNGAC.

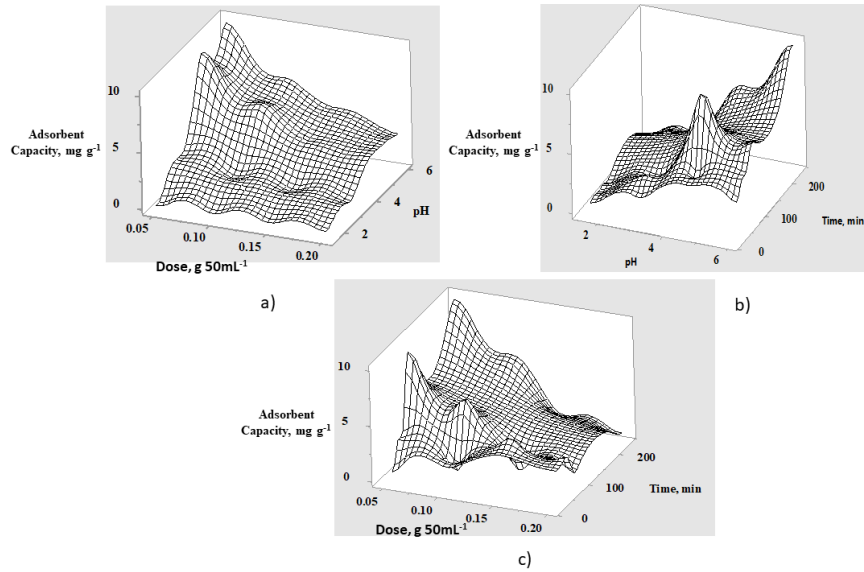


Fig. 6. Plots of simultaneous effect of two factors on lead adsorption onto HNGAC: a) initial pH and dose, b) time and pH and c) time and dose.

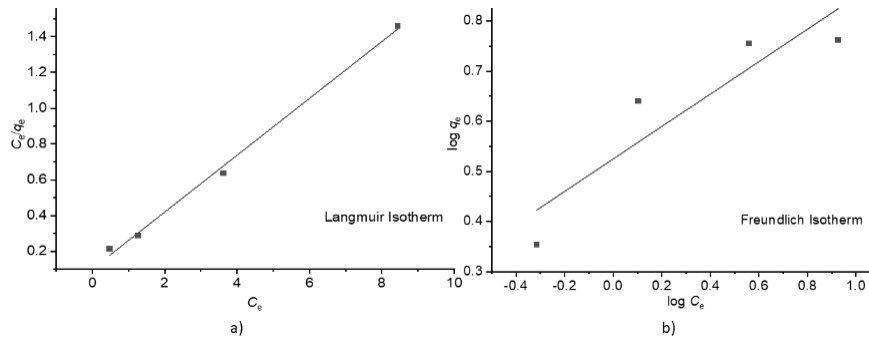


Fig. 7. Isotherm plots for Pb(II) adsorption onto HNGAC: a) Langmuir isotherm and b) Freundlich isotherm (pH 4.5; time 60 min; speed 100 rpm; volume 50 mL; temperature $30 \text{ }^{\circ}\text{C}$; dose 2 g L^{-1}).

TABLE IV. Parameters of the isotherm models for Pb(II) adsorption onto HNGAC.

Langmuir			Freundlich		
$q_m / \text{mg g}^{-1}$	$K_L / \text{L mg}^{-1}$	R^2	$1/n$	$K_F / \text{mg g}^{-1} ((\text{mg L}^{-1})^{1/n})^{-1}$	R^2
9.90099	0.639240506	0.99	0.323	1.688769234	0.836

Kinetic study

Both pseudo-first-order and pseudo-second-order kinetic models were used to assess the adsorption of Pb(II) onto HNGAC. Fig. 8 displays the kinetic plots, while Table V provides the correlation coefficient and kinetic model parameters. Because of its higher correlation coefficient of 0.99, the pseudo-second-order kinetic model better describes the adsorption kinetics than the pseudo-first-order. This implies that chemisorption may play a dominant role in the adsorption process. Compared to the pseudo-first-order model, the value of q_e derived from the pseudo-second-order model agrees better with the experimentally determined q_e value. Abbaszadeh *et al.* observed similar outcomes for the adsorption of Pb(II) on activated carbon from papaya peel biowaste.²⁶ They found a measured uptake capacity of 38.31 mg g^{-1} and a calculated uptake capacity of 42.55 mg g^{-1} from the pseudo-second-order kinetics.

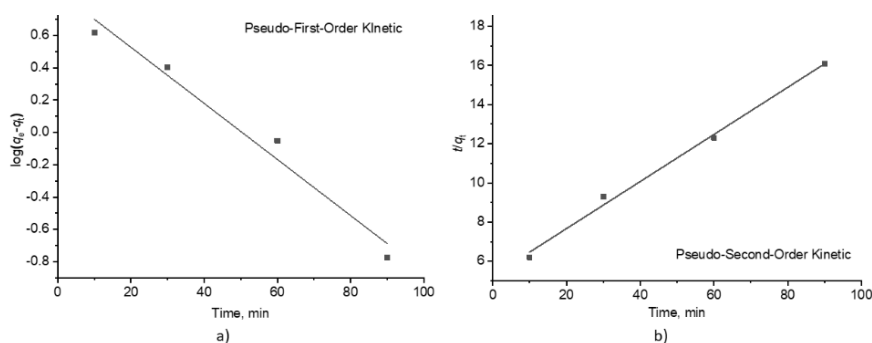


Fig. 8. Kinetic study graph for lead adsorption onto HNGAC: a) pseudo-first-order model and b) pseudo-second-order model (initial pH 4.5; adsorbent dose, $0.1 \text{ g (50 mL)}^{-1}$; Pb(II) concentration, 10.2 mg L^{-1}).

TABLE V. Kinetic model parameters for Pb(II) adsorption onto HNGAC for the PFO and PSO models.

PFO			PSO		
K_1 / h^{-1}	q_e	R^2	$K_2 / \text{g mg}^{-1} \text{h}^{-1}$	q_e	R^2
0.039151	2.394082	0.973	0.002738684	8.333333	0.994

Mechanism of adsorption

The adsorption of Pb(II) onto the adsorbents involves physical and chemical interactions with the surface functional groups. The adsorption of Pb(II) may be caused by ion exchange interactions with surface groups like hydroxyl and carboxyl. The FTIR analysis revealed that the intensity of these groups, especially $-\text{OH}$ and $-\text{COOH}$, was higher in HNGAC compared to GAC, which supports the ion exchange between adsorbent and adsorbate. It was also observed that the amount of Pb(II) uptake by HNGAC was significantly higher than that of GAC, indicating that

chemisorption played a major role in the adsorption process rather than physisorption. Impregnation of GAC with HNO_3 considerably increased the negative surface charge of the adsorbent, which attracted the lead ions.

CONCLUSION

Pb(II) was separated from the effluent of a LAB recycling unit utilizing HNGAC as an adsorbent. The intensity of the $-\text{OH}$ and $-\text{COOH}$ functional groups present on the surface of GAC was found to increase after modification using nitric acid, moreover some new nitrogen-containing functional groups were formed after modification. Modification led to an increase in mesopores and a decrease in micropores. The optimum combination of parameters found using Taguchi analysis was: a time of 240 min, pH 6 and an adsorbent dose of $0.05 \text{ g (50 mL)}^{-1}$. The maximum adsorption capacity of GAC increased due to modification from 7.69 to 9.93 mg g^{-1} . From the isotherm and kinetic studies, it can be inferred that adsorption of lead onto HNGAC follows the Langmuir isotherm and pseudo-second-order kinetics. Adsorption of lead onto HNGAC include monolayer adsorption followed by chemical interaction with functional groups available on the adsorbent surface. Overall, it could be established that, adsorption can be used as an effective technique for the remediation of lead from the wastewater of a lead-acid battery recycling unit and HNGAC could be used as an efficient adsorbent.

Acknowledgements. The authors want to acknowledge the support and facilities provided by National Institute of Technology Raipur, India. The author also wants to acknowledge the Guru Ghasidas University Bilaspur, India, for granting the study leave to do Ph.D.

ИЗВОД

АДСОРПЦИОНО УКЛАЊАЊЕ Рb(II) ИЗ ИНДУСТРИЈСКОГ ЕФЛУЕНТА ПРИМЕНОМ АКТИВНОГ УГЉА МОДИФИКОВАНОГ АЗОТНОМ КИСЕЛИНОМ: ОПТИМИЗАЦИЈА ПРИМЕНОМ ТАГУЧИ МЕТОДЕ

SAURABH MESHAM¹, ANURADHA N JOSHI¹, GAUTAM PRASAD DEWANGAN¹, CHANDRAKANT THAKUR²
и ANUPAM B. SONI²

¹Department of Chemical Engineering, Guru Ghasidas Vishwavidyalaya, Bilaspur, 495009, Chhattisgarh, India и ²Department of Chemical Engineering, National Institute of Technology Raipur, 492010, Chhattisgarh, India

Циљ ове студије био је испитивање примене гранулисаног активног угља модификованог азотном киселином за третман отпадних вода из постројења за рециклажу оловно-киселинских акумулатора, ради уклањања олова. Адсорбенс је окарактерисан применом FTIR, SEM и XRD анализа. Модификацијом су промењене површинске функционалне групе, површинска морфологија и кристалинност. Шаржна адсорпциона испитивања спроведена су ради процене утицаја дозе адсорбенса, почетне рН вредности и контактнoг времена на ефикасност адсорпције уклањања олова. Експерименти су изведени у складу са Тагучи методом дизајна експеримената, а фактори су оптимизовани на основу анализе односа сигнал/шум (SNR) у циљу максимизације одзива. Оптималне вредности фактора утврђене су као рН 6, доза адсорбенса од $0,05 \text{ g}$ и време од 240 min за адсорпцију олова на адсорбенс, при чему је адсорпциони капацитет износио $9,93 \text{ mg g}^{-1}$.

На основу ANOVA анализе, рН је идентификован као најзначајнији фактор, са *F*-вредношћу од 28,07. Изотермска и кинетичка испитивања такође су спроведена ради разумевања механизма адсорпције. Утврђено је да адсорпција прати Лангмуирову изотерму и кинетички модел другог реда.

(Примљено 19. августа, ревидирано 22. октобра, прихваћено 25. децембра 2025)

REFERENCES

1. S. Meshram, R. S. Thakur, G. Jyoti, C. Thakur, A. B. Soni, *J. Indian Chem. Soc.* **99** (2022) 100469 (<https://doi.org/10.1016/j.jics.2022.100469>)
2. M. Caccin, M. Giorgi, F. Giacobbo, M. D. Ros, L. Besozzi, M. Mariani, *Desalin. Water Treat.* **57** (2016) 4557 (<https://doi.org/10.1080/19443994.2014.992974>)
3. S. Meshram, C. Thakur, A. B. Soni, *J. Serb. Chem. Soc.* **85** (2020) 953 (<https://doi.org/10.2298/JSC191103015M>)
4. S. Meshram, S. Dharmadhikari, R. S. Thakur, C. Thakur, A. B. Soni, *J. Hazard. Mater. Adv.* **10** (2023) 10297 (<https://doi.org/10.1016/j.hazadv.2023.100297>)
5. C. Thakur, I. D. Mall, V. C. Srivastava, *Theor. Found. Chem. Eng.* **48** (2014) 60 (<https://doi.org/10.1134/S004057951401014X>)
6. C. P. Dwivedi, J. N. Sahu, C. R. Mohanty, B. R. Mohan, B. C. Meikap, *J. Hazard. Mater.* **156** (2008) 596 (<https://doi.org/10.1016/j.jhazmat.2007.12.097>)
7. J. P. Chen, X. Wang, *Sep. Purif. Technol.* **19** (2000) 157 ([https://doi.org/10.1016/S1383-5866\(99\)00069-6](https://doi.org/10.1016/S1383-5866(99)00069-6))
8. M. A. E. Franco, C. B. Carvalho, M. M. Bonetto, R. P. Soares, L. A. Féris, *J. Clean. Prod.* **161** (2017) 947 (<https://doi.org/10.1016/j.jclepro.2017.05.197>)
9. A. H. Sulaymon, D. W. Abood, A. H. Ali, *Hydrol. Curr. Res.* **2** (2011) 1000120 (<http://dx.doi.org/10.4172/2157-7587.1000120>)
10. A. Jusoh, L. S. Shiung, N. Ali, M. J. M. M. Noor, *Desalin.* **206** (2007) 9 (<https://doi.org/10.1016/j.desal.2006.04.048>)
11. K. Wang, J. Zhao, H. Li, X. Zhang, H. Shi, *J. Taiwan Inst. Chem. Eng.* **61** (2016) 287 (<https://doi.org/10.1016/j.jtice.2016.01.006>)
12. H. J. Fan, P. R. Anderson, *Sep. Purif. Technol.* **45** (2005) 61 (<https://doi.org/10.1016/j.seppur.2005.02.009>)
13. S. Yao, J. Zhang, D. Shen, R. Xiao, S. Gu, M. Zhao, J. Liang, *J. Colloid Interface Sci.* **463** (2016) 118 (<https://doi.org/10.1016/j.jcis.2015.10.047>)
14. Z. Jiang, Y. Liu, X. Sun, F. Tian, F. Sun, C. Liang, W. You, C. Han, C. Li, *Langmuir* **19** (2003) 731 (<https://doi.org/10.1021/la020670d>)
15. A. M. El-Wakil, W. M. Abou El-Maaty, F. S. Awad, *J. Anal. Bioanal. Tech.* **5** (2014) 1000187 (<https://doi.org/10.4172/2155-9872.1000187>)
16. M. Nandhini, B. Suchithra, R. Saravanathamizhan, D. G. Prakash, *J. Electrochem. Sci. Eng.* **4** (2014) 227 (<https://doi.org/10.5599/jese.2014.0056>)
17. S. Meshram, C. Thakur, A. B. Soni, *Pollution* **6** (2020) 879 (<https://doi.org/10.22059/poll.2020.302442.808>)
18. M. A. Ramos, V. G. Serrano, C. V. Calahorra, A. J. L. Peinado, *Spectrosc. Lett.* **26** (1993) 1117 (<https://doi.org/10.1080/00387019308011598>)
19. V. G. Serrano, M. A. Ramos, A. J. L. Peinado, C. V. Calahorra, *Thermochim. Acta* **291** (1997) 109 ([https://doi.org/10.1016/S0040-6031\(96\)03098-5](https://doi.org/10.1016/S0040-6031(96)03098-5))

20. V. C. Srivastava, I. D. Mall, I. M. Mishra, *J. Hazard. Mater.* **134** (2006) 257 (<https://doi.org/10.1016/j.jhazmat.2005.11.052>)
21. T. S. Anirudhan, S. S. Sreekumari, *J. Environ. Sci.* **23** (2011) 1989 ([https://doi.org/10.1016/S1001-0742\(10\)60515-3](https://doi.org/10.1016/S1001-0742(10)60515-3))
22. N. A. Kolar, S. Sharifian, T. Kaghazchi, *Turkish J. Chem.* **43** (2019) 663 (<https://doi.org/10.3906/kim-1810-63>)
23. M. Dutta, S. Mishra, M. Kaushik, J. K. Basu, *Res. J. Environ. Sci.* **5** (2011) 741 (<https://doi.org/10.3923/rjes.2011.741.751>)
24. X. Jiang, X. Lan, Y. Song, X. Xing, H. M. A. Hassan, *J. Chem.* (2019) 8593742 (<https://doi.org/10.1155/2019/8593742>)
25. M. Calero, A. Pérez, G. Blázquez, A. Ronda, M. A. M. Lara, *Ecol. Eng.* **58** (2013) 344 (<https://doi.org/10.1016/j.ecoleng.2013.07.012>)
26. S. Abbaszadeh, S. R. W. Alwi, C. Webb, N. Ghasemi, I. I. Muhamad, *J. Clean. Prod.* **118** (2016) 210 (<https://doi.org/10.1016/j.jclepro.2016.01.054>)
27. Z. Guo, J. Zhang, Y. Kang, H. Liu, *Ecotoxicol. Environ. Saf.* **145** (2017) 442 (<https://doi.org/10.1016/j.ecoenv.2017.07.061>)
28. Y. Li, Q. Du, X. Wang, P. Zhang, D. Wang, Z. Wang, Y. Xia, *J. Hazard. Mater.* **183** (2010) 583 (<https://doi.org/10.1016/j.jhazmat.2010.07.063>)
29. S. Meshram, C. Thakur, A. B. Soni, *Indian Chem. Eng.* **63** (2020) 460 (<https://doi.org/10.1080/00194506.2020.1795933>).